inorganics

MDPI

Article

Spectroscopic, Anti-Cancer Activity, and DFT Computational Studies of Pt(II) Complexes with 1-Benzyl-3-phenylthiourea and Phosphine/Diamine Ligands

Dina Saadi Mohamed [1], Subhi A. Al-Jibori [2], Reza Behjatmanesh-Ardakani [3], Ahmed S. Faihan [2], Tarek A. Yousef [4,5], Abdulrahman G. Alhamzani [4], Mortaga M. Abou-Krisha [4,6], Ahmed S. M. Al-Janabi [2,*] and Benjamin S. Hsiao [7]

1 Department of Chemistry, College of Education for Women, University of Tikrit, Tikrit 34001, Iraq
2 Department of Chemistry, College of Science, University of Tikrit, Tikrit 34001, Iraq
3 Department of Chemistry, Payame Noor University, Tehran 19395-4697, Iran
4 Chemistry Department, College of Science, Imam Mohammad Ibn Saud Islamic University (IMSIU), Riyadh 11623, Saudi Arabia
5 Department of Toxic and Narcotic Drug, Forensic Medicine, Mansoura Laboratory, Medicolegal Organization, Ministry of Justice, Mansoura 11001, Egypt
6 Department of Chemistry, South Valley University, Qena 83523, Egypt
7 Department of Chemistry, Stony Brook University, Stony Brook, New York, NY 11794-3400, USA
* Correspondence: dr.ahmed.chem@tu.edu.iq

Abstract: The reaction between $[PtCl_2(L\text{-}L)]$ (L-L = dppe, dppp, dppb, dppf, Phen and Bipy) or $[PtCl_2(PPh_3)_2]$ with 1-benzyl-3-phenylthiourea (H_2BPT) in a basic medium ($CHCl_3$/EtOH) created new coordinated square planner Pt(II) complexes with [Pt(BPT)(L-L)] (**1**–**4**,**6**,**7**) and $[Pt(BPT)(PPh_3)_2]$ (**5**) types. These complexes were fully characterized by analytical and spectroscopic techniques (i.e., IR, UV. Vis., ^1H, and ^{31}P NMR). The results indicated that the thiourea derivative ligand act as a dianion ligand bonded through both S and N atoms in a chelating mode or as a mono-anion ligand coordinated through a sulfur atom with Pt(II) ion. Cytotoxicity activity was performed by the MTT assay to determine anti-cancer activities against MCF-7 breast cancer cells. The study indicated that IC_{50} values for MCF-7 cells were 10.96–78.90 μM. Additionally, the complexes [Pt(BPT)(dppe)] (**1**), $[Pt(BPT)(PPh_3)_2]$ (**5**), and $[Pt(BPT)_2(Bipy)]$ (**7**) were investigated theoretically, where their quantum parameters were evaluated using the Gaussian 09 program using the theory of B3LYP/Def2TZVP//B3LYP/Lanl2dz. The calculation results confirmed the optimized structures of the complexes square planar geometry. However, the calculated bond lengths and angles showed a slightly distorted square planar geometry due to the *trans* influence of the sulfur atom. Additionally, complexes of [Pt(BPT)(dppe)] (**1**) and $[Pt(BPT)(PPh_3)_2]$ (**5**) showed higher stability compared to $[Pt(BPT)_2(Bipy)]$ (**7**), which can be attributed to the higher back-donation of (**1**) and (**5**) complexes. Furthermore, among the three complexes, the $[Pt(BPT)_2(Bipy)]$ (**7**) complex possessed the lowest HOMO–LUMO gap, which may be a good candidate as the photo-catalyst material.

Keywords: thiourea; phosphine; computational; DFT; platinum

Citation: Mohamed, D.S.; Al-Jibori, S.A.; Behjatmanesh-Ardakani, R.; Faihan, A.S.; Yousef, T.A.; Alhamzani, A.G.; Abou-Krisha, M.M.; Al-Janabi, A.S.M.; Hsiao, B.S. Spectroscopic, Anti-Cancer Activity, and DFT Computational Studies of Pt(II) Complexes with 1-Benzyl-3-phenylthiourea and Phosphine/Diamine Ligands. *Inorganics* **2023**, *11*, 125. https://doi.org/10.3390/inorganics11030125

Academic Editor: Carlos Martínez-Boubeta

Received: 4 February 2023
Revised: 24 February 2023
Accepted: 1 March 2023
Published: 16 March 2023

1. Introduction

Thioureas have received great research interest due to their diverse potential applications. Thioureas are known to bind to metal ions and form multiple coordination geometries [1,2], where the mono-anion ligand is considered one of the best-known scenarios in thioureas complexes. Another type of coordination can also occur when thioureas are attached to metal ions as neutral ligands. Di-anionic ligands are also possible but are the least likely form of thiourea complexes. Benzoyl thiourea, a special type of thiourea, can interact with transition metal centers through S, O, and N atoms [3–5]. Thiourea-metal

complexes have been utilized in different applications [6–12], such as heavy metal separation [6], nano-materials precursor preparation [7], and biologically active materials. In the case of biologically active materials, glutathione, a thiourea derivative, is an interesting compound because it is present in biological systems and can be exploited as practical sulfur-containing nucleophiles [13–18].

In other biological active systems, platinum-acyl-thiourea complexes have been demonstrated as materials with antifungal and virus-inhibitory capabilities [16]. However, a detailed investigation of the composition, biological activity, and stability of thiourea derivatives in these systems is yet to be made. In this study, an in-depth investigation was carried out in this system, where the understanding could lead to the creation of stronger antibacterial drugs. Specifically, thiourea derivative metal (Pt(II)) complex ligands were investigated. The study included the synthesis, characterization, and antibacterial properties of 1-benzyl-3-phenylthiourea ligands and associated platinum metal complexes, which have never been reported.

2. Results

2.1. Synthesis

The schematic diagram of the ligand 1-benzyl-3-phenylthiourea (H_2BPT) synthesis is illustrated in Scheme 1. This H_2BPT ligand was subsequently reacted with the following agents: tertiary phosphine and amine ligands: [$PtCl_2$(diphos)], [PCl_2(Phen)], and [$PtCl_2$(Bipy)] in a molar ratio (1:2) in the presence of a base medium to prepare Pt(II) complexes in a dianion form, where the varying synthetic pathways are shown in Schemes 2–4.

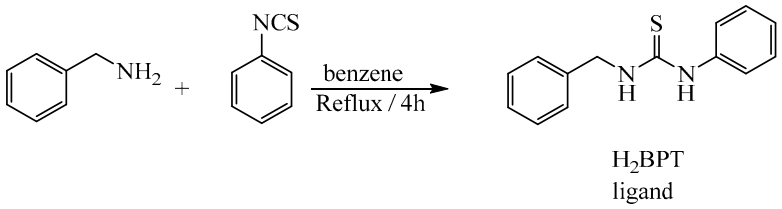

Scheme 1. Preparation of 1-benzyl-3-phenylthiourea.

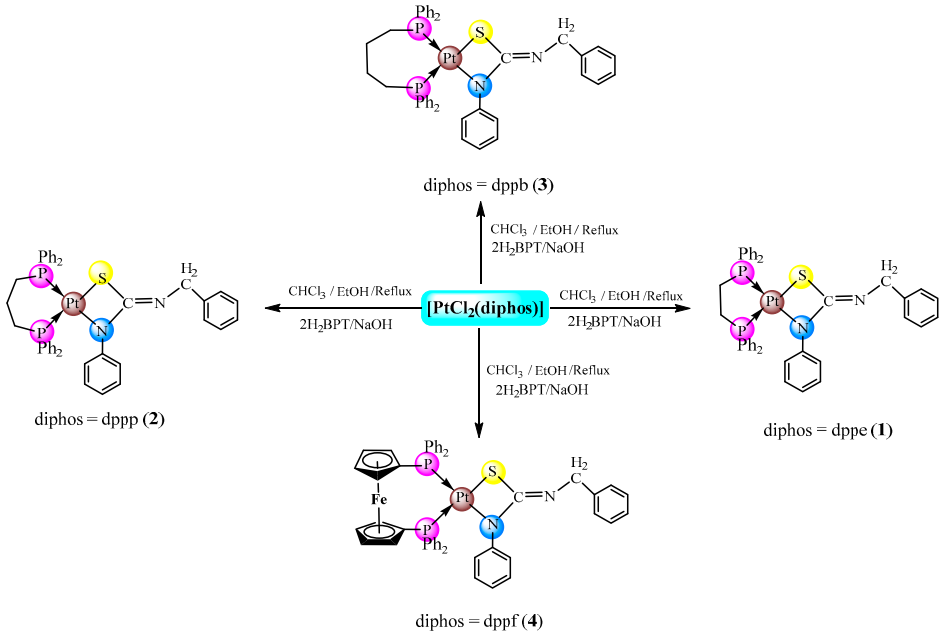

Scheme 2. Preparation of the complexes (**1**–**4**).

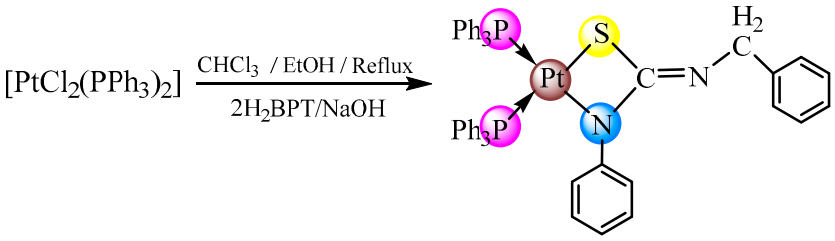

Scheme 3. Preparation of the complex (**5**).

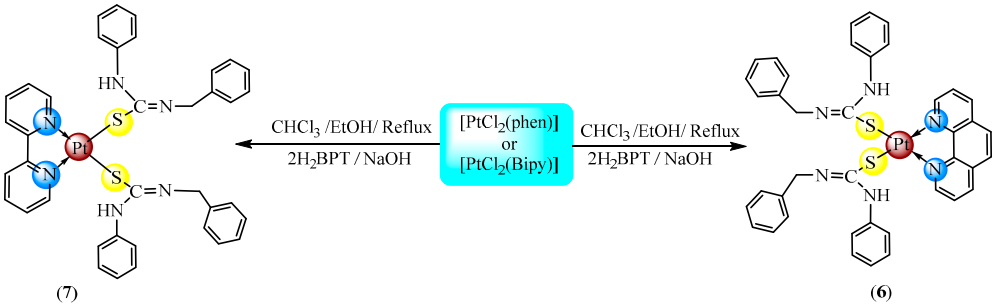

Scheme 4. Preparation of the complexes (**6** and **7**).

The conductivity measurements of the complexes (**1**–**7**) in DMSO solvent showed that these complexes are non-electrolytes [19]. The CHN analysis was carried out, where the results (Table 1) are in good agreement with the suggested structures of the prepared compounds.

Table 1. Melting point (m.p., °C), yield (%), color, conductivity, and CHN analysis of the H_2BPT ligand and its complexes.

No.	Complexes	Color	Yield (%)	m.p. (°C)	Λ_M ($ohm^{-1}\cdot cm^2\cdot mole^{-1}$)	Elemental Analysis (%) Found (Calc.)		
						C	H	N
	H_2BPT	white	90	167–169		69.39(69.20)	5.82(5.89)	11.56(11.68)
1.	[Pt(BPT)(dppe)]	off-white	64	290–295	1.3	57.62(57.92)	4.35(4.61)	3.36(3.40)
2.	[Pt(BPT)(dppp)]	yellow	72	220–223	4.5	58.08(57.93)	4.52(4.47)	3.30(3.42)
3.	[Pt(BPT)(dppb)]	yellow	78	271–273	6.3	58.53(58.67)	4.68(4.59)	3.25(3.37)
4.	[Pt(BPT)(dppf)]	yellow	70	245–248	11.5	58.25(58.35)	4.07(4.30)	2.83(3.08)
5.	$[Pt(BPT)(PPh_3)_2]$	Yellow	72	210–212	3.4	62.56(62.74)	4.41(4.70)	2.92(3.11)
6.	$[Pt(BPT)_2(Phen)]$	Brown	72	208–211	2.6	56.00(55.86)	3.99(4.08)	9.80(9.91)
7.	$[Pt(BPT)_2(Bipy)]$	Brown-red	80	214–217	6.9	54.73(54.88)	4.11(4.22)	10.08(10.23)

2.2. Spectroscopic Investigation

2.2.1. IR Spectra

The IR spectra of 1-benzyl-3-phenylthiourea (H_2BPT) ligand showed the amide absorption bands at (3149) and (3363) cm^{-1} and thioamide bands at (1450) cm^{-1} and (842) cm^{-1} [20–23]. However, the complexes (**1**–**7**) showed no N–H absorption bands as in H_2BPT. The stretching vibration of S–C=N was identified in the range of (1539–1566) cm^{-1}, indicating the presence of ionic interaction between the ligand and the central metal ion. Interestingly, tertiary phosphine ligands could be found upon the coordination between the ligand, and Pt(II) ion as seen by the appearance of the Ph-p and C-p bands in the IR spectra, such as the υ (P–C) absorption peaks appeared at (505–536) cm^{-1} and (1099–1103) cm^{-1}, respectively [24–28], as well as the υ (P–Ph) peak appeared in the range of (1433–1435) cm^{-1}. Other IR bands are listed in Table 2.

Table 2. Characteristic peaks in the IR spectra for the synthesized complexes (**1**–**7**) and the ligand H_2BPT.

Compounds	υ (N–H)	υ (C–H) Aromatic	υ (C–H) Aliphatic	υ (S–C=N)	υ (C–S)	Phosphine		
						υ (P–C) Bending	υ (P–C)	υ (P–Ph)
H_2BPT	3149 3363	3060	2974	1450	842	———	———	——-
1	——	3053	2924	1541	746	534	1103	1435
2	——	3051	2922	1546	746	511	1101	1433
3	——	3053	2928	1566	742	505	1099	1433
4	——	3053	2916	1566	744	563	1099	1435
5	——	3053	2922	1541	744	545	1095	1433
6	3147	3030	2976	1539	738	——	——	——
7	3153	3049	2916	1541	761	——	——	——

2.2.2. ^{1}H and ^{31}P-{^{1}H}, ^{13}C-{^{1}H} NMR Spectra

The presence of the two singlets at δ = 9.627 (*s*, 1H) and δ = 8.164 (*s*, 1H) could be attributed to the two N–H groups in the H_2BPT ligand. Protons of the aromatic rings showed one triplet at δ = 7.118 (*t*, 1H, J_{HH} = 6.78 Hz), whereas the other phenyl protons showed an unresolved multiplet in the range of δ = 7.439–7.258 (*m*, 9H). The methylene proton displayed as a doublet at δ = 7.37 (*d*, 1H, J_{HH} = 7.40 Hz). (Figure S1, Supporting Information).

In the ^{1}H NMR spectra, complexes (**1**–**5**) (Figures S2–S6, Supporting Information) exhibited no N–H signals when the compound was modified by NaOH. Complexes (**6**) and (**7**) showed that one proton was removed from the NH group, indicating the bonding of the two HBPT ligands on the side of the sulfur atom with the Pt(II) ion. A set of signals was seen within the 7–7.5 ppm range, which belongs to the phenyl groups for the phosphine ligands and the BPT^{-2} ligand. The protons of the aromatic rings for both BPT^{-2} and the phosphine ligands were shown as broad peaks within the 6–8 ppm range. On the other hand, the aliphatic protons of the phosphine ligands were shown within 1–4 ppm. Likewise, the Cp ring of the dppf ligand displayed two distinctive singlets at δ = 4.08 and 4.29 ppm, respectively. The protons of Phen and Bipy in the ^{1}H NMR spectra of complexes (**6** and **7**) (Figures S7 and S8, Supporting Information) displayed as distinctive four peaks. For the Phen ligand in complex (**6**), these four peaks appeared at δ = 7.86 (*d*, 2H), 8.34 (*s*, 2H), 8.72 (*dd*, 2H,), and 9.80 (*d*, 1H) ppm, whereas for the Bipy ligand in complex (**7**), the four peaks appeared at δ = 7.76 (*d*, 2H), 7.97 (*d*, 2H), 8.19 (*t*, 2H), and 8.48 (*d*, 1H) ppm.

The ^{31}P-{^{1}H} NMR spectra of the complexes (**1**–**5**) (Figures S9–S13, Supporting Information) revealed the AX pattern, where two doublets from the platinum satellites appeared. The spectrum of the complex (**1**) showed two doublets at *δ* = 43.26 and 49.88 ppm in a 1:1 ratio with a coupling constant of J_{PP} 5.7 Hz. Moreover, the platinum satellites associated with complex (**1**) at 2884 and 5386 Hz. The split pattern indicates that the Pt(II) ion is attached to both S and N donor atoms in a chelating fashion, where the sulfur atom is trans to one phosphorus atom and the nitrogen atom is trans to the other phosphorus atom [24–26]. The remaining mixed ligand phosphine complexes of Pt(II) have a similar pattern and can be explained accordingly.

The ^{13}C-NMR spectrum of the H_2BPT ligand is in good agreement with the suggested structure since H_2BPT has ten different types of carbon atoms (see Figure S14 Supporting Information). Two significant peaks in the ^{13}C NMR spectrum are the carbon peaks of the C=S group at δ185.01 ppm, and the methylene group (NH-**C**H_2-) displayed at δ55.63 ppm. At the same time, the other phenyl carbons showed eight peaks in the range of δ = 146.92–122.36 ppm.

The formation of complexes (**1**, **2**, **6,** and **7**) (Figures S15–S18 Supporting Information) was supported by ^{13}C-{^{1}H} NMR spectra which showed the chemical shift of the carbon atoms of the C=S group and the methylene group (NH-**C**H_2-) in low-frequency peaks with

δ 172.63–178.63 ppm. These recorded shifts reflected a down-field shift of about 7–13 ppm from the free thiourea ligand, suggesting decreased electron density on the thiocarbonyl carbon, and the coordination happened through a sulfur atom. In a similar view, the chemical shift of the methylene group (NH-$\underline{C}H_2$-) was shifted down-field, which showed at δ 49.06–53.98 ppm. The spectra of complexes (**1** and **2**) displayed the chemical shift of the carbons of the aliphatic group (CH_2) at δ 31.23 ppm and (δ 19.09 and δ 31.23) ppm, respectively. In addition, the spectra of the complexes (**6** and **7**) displayed the chemical shift of the carbon of the (C=N) group of diamine ligands at δ 156.81 ppm and δ 155.75 ppm, respectively. Other chemical shifts are listed in Table 3.

Table 3. ^{31}P-{^{1}H}, ^{13}C-{^{1}H}**,** and ^{1}H-NMR chemical shifts for the synthesized complexes (**1**–**7**) and the H_2BPT ligand.

Comps.	Chemical Shifts δ (ppm)
H_2BPT	**^{1}H NMR**: 4.74 (*d*, 2H, CH_2), 7.118 (*t*, 1H, J_{HH} = 6.78 Hz), 7.258–7.439 (*m*, 9H, H-Phenyl), 8.16 (*s*, 1H, NH), 9.63 (*s*, 1H, NH). **^{13}C-{^{1}H}NMR**: 185.01(C=S), (146.92, 133.68, 132.41, 131.04, 130.08, 129.34, 128.83, 122.36) aromatic carbons, 55.63 (NH-$\underline{C}H_2$-)
1	**^{31}P-{^{1}H}NMR**: P_A = 49.88 (*d*, $^2J_{PA-PX)}$ = 5,7 H_Z, J_{Pt-PA} = 5386 H_Z), δP_A = 43.26 (d, $^2J_{PA-PX)}$ = 5.7 H_Z, J_{Pt-PA} = 2884 H_Z) **^{1}H NMR**: 2.48 (*s*, 4H, 2CH_2-dppe), 7.08–7.83 (*m*, 20H, H-Phenyl), 4.72 (*s*, 2H, CH_2). **^{13}C-{^{1}H}NMR**: 178.64(C=S), (147.98, 144.14, 139.87, 135.56, 134.45, 133.13, 132.19, 130.90, 129.77, 129.30, 129.20, 128.30) aromatic carbons, 53.98 (NH-$\underline{C}H_2$-), 31.23 ($\underline{C}H_2$-dppe)
2	**^{31}P-{^{1}H}NMR**: δP_A = 1.205 (*d*, $^2J_{(PA-PX)}$ = 32.4 H_Z, J_{Pt-PA} = 7244 H_Z), δP_X = −5.76 [*d*, $^2J_{(PX-PA)}$ = 32.4 H_Z, J_{Pt-PX} = 9769 H_Z) **^{1}H NMR**: 1.71 (*m*, 2H, CH_2-dppp), 2.82 (*m*, 4H, CH_2-dppp), 4.73 (*s*, 2H, CH_2), 7.07–7.74 (*m*, 30 H, H-Phenyl). **^{13}C-{^{1}H}NMR**: 172.63(C=S), (147.24, 142.07, 135.16, 134.63, 133.71, 132.44, 131.07, 131.03, 131.00, 129.80, 129.42, 129.33, 128.65, 125.61, 123.38) aromatic carbons, 49.78 (NH-$\underline{C}H_2$-), 31.23 (P$\underline{C}H_2$-dppp), 19.09 ($\underline{C}H_2$-dppp)
3	**^{31}P-{^{1}H}NMR**: δP_A = 15.15 (*d*, $^2J_{(PA-PX)}$ = 24.8 H_Z, J_{Pt-PA} = 6383 H_Z), δP_X = 11.22 [*d*,$^2J_{(PX-PA)}$ = 24.8 H_Z, J_{Pt-PX} = 6488 H_Z) **^{1}H NMR**: 2.59 (*s*, 4H, 2CH_2–dppb), 3.04 (*s*, 4H, 2CH_2–dppb), 4.70 (*s*, 2H, CH_2), 7.29–7.67 (*m*, 30H, H-Phenyl).
4	**^{31}P-{^{1}H}NMR**: δP_A = 18.035 (*d*, $^2J_{(PA-PX)}$ = 21.01 H_Z, J_{Pt-PA} = 7764 H_Z), δP_X = 13.505 [*d*, $^2J_{(PX-PA)}$ = 21.01 H_Z, J_{Pt-PX} = 3191 H_Z) **^{1}H NMR**: 4.08 (*s*, 4H, Cp), 4.28 (*s*, 4H, CP), 4.73 (*s*, 2H, CH_2), 6.60–7.32 (*m*, 30H, H-Phenyl)
5	**^{31}P-{^{1}H}NMR**: δP_A = 29.99 (*d*, $^2J_{(PA-PX)}$ = 22.9 H_Z, J_{Pt-PA} = 2314 H_Z), δP_X = 19.63 [*d*, $^2J_{(PX-PA)}$ = 22.9 H_Z, J_{Pt-PX} = 2460 H_Z) **^{1}H NMR**: 4.72 (*s*, 2H, CH_2), 6.91–7.72 (*m*, 40H, H-Phenyl).
6	**^{1}H NMR**: 4.70 (*s*, 2H, CH_2), 7.00–7.55 (*m*, 20H, H-Phenyl), 7.86 (*d*, 2H, J_{HH} = 6.23 Hz, H-Phen), 8.34 (*s*, 2H, H-Phen), 8.72 (*dd*, 2H, J_{HH} = 6.48 Hz, H-Phen), 9.42 (*s*, 2H, NH), 9.80 (*d*, 1H, J_{HH} = 7.80 Hz, H-Phen). **^{13}C-{^{1}H}NMR**: 173.36(C=S), 156.81(C=N), (152.07, 144.92, 142.04, 135.85, 133.84, 132.65, 129.96, 128.61, 125.89, 125.06) aromatic carbons, 49.06 (NH-$\underline{C}H_2$-).
7	**^{1}H NMR**: 4.70 (*s*, 2H, CH_2), 7.09–7.45 (*m*, 20H, H-Phenyl), 7.76 (*d*, 2H, J_{HH} = 7.80 Hz, H-Bipy), 7.97 (*d*, 2H, J_{HH} = 7.60 Hz, H-Bipy), 8.19 (*t*, 2H, J_{HH} = 7.90 Hz, H-Bipy), 8.48 (*d*, 1H, J_{HH} = 8.00 Hz, H-Bipy), 9.09 (*s*, 2H, NH). **^{13}C-{^{1}H}NMR**: 174.05(C=S), 155.75(C=N), (146.92, 140.92, 132.41, 131.08, 131.00, 130.08, 129.48, 129.34, 129.30, 128.83, 122.36, 120.21) aromatic carbons, 52.54 (NH-$\underline{C}H_2$-).

2.2.3. UV–Visible Spectra

In the electronic absorption spectra of Pt(II) square planar complexes, the first spin allowed the d-d transition ($^1A_1g \rightarrow {}^1A_{2g}$) for Pt(II), where the transition could be identified at 420–480 cm^{-1} [29]. In addition, the electronic spectrum of the Pt(II) complexes (**1–7**) could display absorption bands between 20,833 and 23,809 cm^1 due to the $^1A_1g \rightarrow {}^1A_{2g}$ transition (Table 4 and Figure 1).

Table 4. Characteristic values in the UV–visible spectra of the planar square Pt(II) complexes.

Complexes	λ_{max} (nm)
1	420
2	446
3	452
4	480
5	475
6	464
7	460

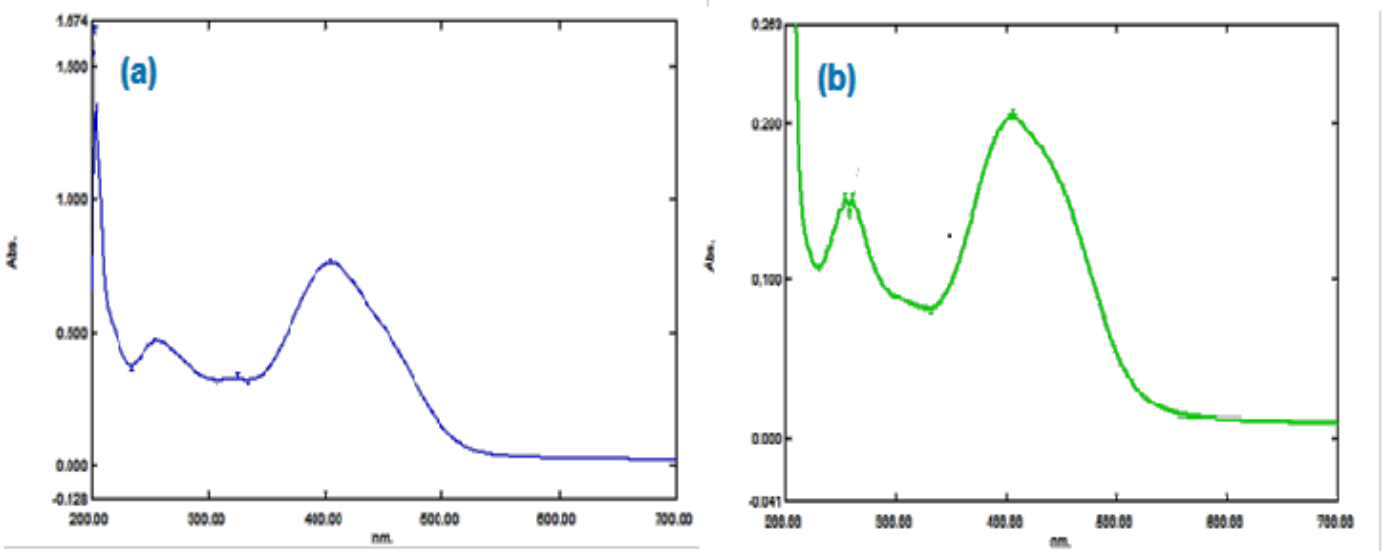

Figure 1. UV–Visible spectra complexes of the complexes (**a**) [Pt(BPT)(dppe)], and (**b**) [Pt(BPT)(dppb)].

2.3. Cytotoxicity of Selective Complexes

The cytotoxicity of the ligand and two selective complexes (**4** and **6**) was examined against breast carcinoma (MCF-7 cancer cells) using the MTT assay. The IC_{50} value (IC_{50} is the concentration that inhibits 50% of the MCF-7 cell growth) was determined by the method, where the results are summarized in Table 5. From this table, the following features were observed.

Table 5. The IC_{50} values of the tested complexes against MCF-7 cancer cells.

Pt(II) Complex	IC_{50} (μM) *
[Pt(BPT)(dppe)]	78.90 ± 2.87
[Pt(BPT)(dppb)]	47.07 ± 1.89
$[Pt(BPT)_2(Phen)]$	10.96 ± 1.12
Cis-platin	7.96 ± 0.69

* IC50(μM): 1–10 (very strong), 11–25 (strong), 26–50 (moderate), 51–100 (weak), above 100 (non-cytotoxic) [30].

- Complex (**6**) exhibited the highest activity towards MCF-7 cells with an IC_{50} value of 10.96 ± 1.12 µM, indicating that complex (**6**) could be used chemotherapeutically.
- Complex (**4**) revealed moderate activity toward MCF-7 cell lines with an IC_{50} value of 47.07 ± 1.89 µM.
- The free H_2BPT ligand exhibited weak efficacy towards MCF-7 cancer cells with an IC_{50} value of 78.90 ± 2.87 µM.
- The efficacy of the best-performing complex (**6**), Pt(BPT)$_2$(Phen) is approaching the common cancer drug Cis-platin.

2.4. Computational Studies

2.4.1. Geometrical and Electronic Properties

The optimized structures of [Pt(BPT)(dppe)] (**1**), [Pt(BPT)(PPh_3)$_2$] (**5**), and [Pt(BPT)$_2$(Bipy)] (**7**) complexes show that the thiourea ligand with a −2 charge can coordinate to the platinum central atom through its S^- and N^- atoms. The final optimized geometries for these three complexes are square planar symmetry, with Pt(II) at the center, attached to P, S, and N atoms (Figure 2). The calculated bond length shows that not all four bonds to the Pt(II) are equivalent. For example, the bond distance of Pt–N possesses a shorter bond length than those of Pt–S and Pt–P. Moreover, the two phosphorus atoms that attach to the Pt(II) atom are non-equivalent. One of the Pt-P bonds has a bond length of 2.42 Å while the other has a bond length of 2.37 Å. These values are consistent with our previous work [31], which displayed the Pt-P lengths as 2.233 Å and 2.264 Å, respectively. Furthermore, it is worth mentioning that when the tertiary phosphine ligand is replaced, the Pt-P bond length can also change. These differences can be attributed to the slightly straightened ring for the dppe ligand (complex (**1**)) and the PPh_3 ligand (complex (**5**)). The change in the Pt-P bond length in these complexes can be attributed to the stronger trans influence of the S atom compared to the N atom [32]. The Pt-P bond that is trans to the sulfur atom has a longer bond length, whereas the Pt-P bond that is trans to the nitrogen atom has a shorter bond length. In addition, the bond length of Pt–S in these three complexes showed a constant value of about 2.42 Å, but the bond length of Pt–N has different values. In complexes (**1**, **5**, and **7**), the Pt-N bond lengths are 2.06, 2.07, and 2.08 Å, respectively. The average bond length of Pt–P in [Pt(BPT)(dppe)] (**1**) is shorter than the average bond length of Pt–P in [Pt(BPT)(PPh_3)$_2$] (**5**). The ligand field theory predicts that Pt(II), d^8 has a square planar symmetry. However, the calculated bond angles are not equal to 90°, indicating a slightly distorted square planar geometry. For example, in complex [Pt(BPT)(dppe)] (**1**), the bond angle of P–Pt–P is 85.4°, while in [Pt(BPT)(PPh_3)$_2$] (**5**), the bond angle is 100°. On the other hand, the bond angles in N–Pt–S are 71.2° and 70.7° for [Pt(BPT)(dppe)] (**1**) and [Pt(BPT)(PPh_3)$_2$] (**5**), respectively.

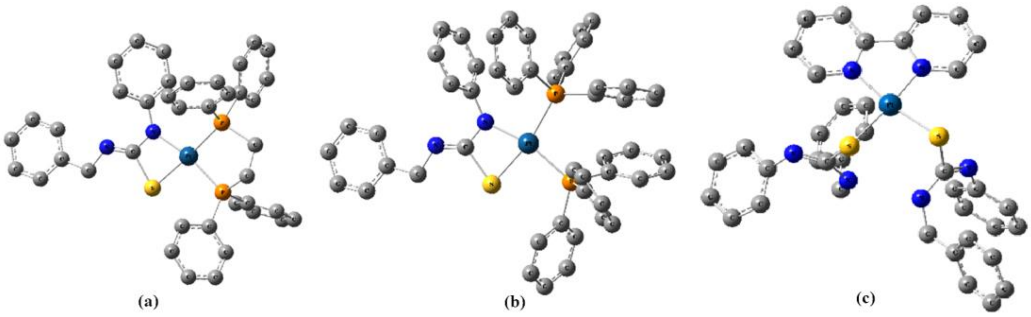

Figure 2. Optimized structures for (**a**) [Pt(BPT)(dppe)] (**1**), (**b**) [Pt(BPT)(PPh_3)$_2$] (**5**), (**c**) [Pt(BPT)$_2$(Bipy)] (**7**). Hydrogen atoms were not shown for simplicity.

The highest occupied molecular orbital (HOMO) and the lowest unoccupied molecular orbital (LUMO) were calculated at the level of B3LYP/Def2-TZVP (Figure 3). It was found that the HOMO–LUMO gap for [Pt(BPT)$_2$(Bipy)] (**7**) is less than the two other complexes. These results suggest that [Pt(BPT)$_2$(Bipy)] (**7**) may be considered as a photocatalyst with

electron-hole activation in the solar energy range. Figure 3 shows that HOMO and LUMO are hybridized orbitals that contain Pt d-orbitals. P atoms have less electronegativity compared to S and N atoms. Therefore, unlike their contribution to LUMO, the P atoms do not contribute to HOMO charge density.

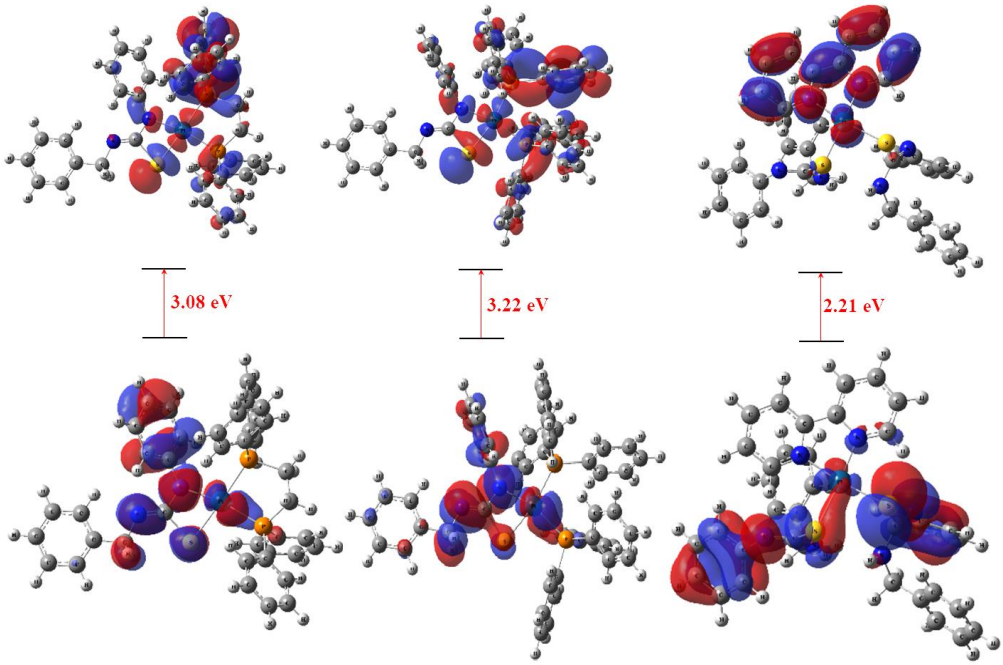

Figure 3. HOMO and LUMO for (**a**) [Pt(BPT)(dppe)] (**1**), (**b**) [Pt(BPT)(PPh_3)$_2$] (**5**), (**c**) [Pt(BPT)$_2$(Bipy)] (**7**).

2.4.2. NBO Analysis

The natural bond orbital (NBO) charges for essential atoms in the complexes were also investigated, and the results are listed in Table 6. In all three complexes, the charge on the central Pt atom ranges from +2 to a much less positive value. These results represent a ligand-to-metal charge transfer. The NBO charges on N and S atoms are negative but less than unity, which indicates that these atoms donate their valence charge to the Pt(II) atom. The charge donation from the sulfur atom has a higher contribution to the Pt(II) atom than the N atom due to the electronegativity difference between N and S atoms (S is softer than N). The obtained data show that the central metal in both complexes (**1**) and (**5**) have less positive charge than complex (**7**), indicating a higher electron donation to Pt(II). These results suggest that P-containing complexes are more stable than N-complexes due to the high electron contribution from the P atoms to the central Pt ion. The electronegativity of P is less than N, S, and even Pt atoms. Even though P atoms displayed positive values in Table 6, there should be a second test by the second-order perturbation energy ($E^{(2)}$) in the NBO analyses. Tables 7–9 show the results of the second-order perturbation energies due to the charge transfer from donor orbitals to the acceptor ones.

Table 6. NBO Charges for the selective complexes (**1**, **5**, and **7**).

Complex	N	N	P	P	S	Pt
(**1**)	−0.68 [1]	−0.55	+1.02 [2]	+0.98	−0.33	+0.31
(**5**)	−0.70 [1]	−0.55	+1.01 [2]	+0.97	−0.30	+0.31
(**7**)	−0.42 [1]	−0.63 [4]	−0.42 [3]	−0.25 [5]	−0.26	+0.53

[1]: for N atom connected to Pt, [2]: for P atom nearest to S, [3]: for the other N atom connected to Pt, [4]: for N in NH group. The other N has −0.66 charge, [5]: for S atom connected to Pt.

Table 7. Second-order perturbation energies ($E^{(2)}$) for charge transfers from donor to acceptor orbitals in Pt(BPT)(dppe)] (**1**).

	Donor	Type	Acceptor	Type	$E^{(2)}$
Donation	$(LP1)_{P30}$	57%(*s*) + 43%(*p*)	Pt27–S28	σ*	159.1
	$(LP2)_{S28}$	100%(*p*)	C32–N39	π*	17.4
	$(LP1)_{P30}$	57%(*s*) + 43%(*p*)	Pt27–P25	σ*	30.8
	$(LP1)_{N39}$	33%(*s*) + 67%(*p*)	C32–S28	σ*	24.6
	$(LP1)_{N40}$	4%(*s*) + 96%(*p*)	Pt27–P25	σ*	12.9
	$(LP1)_{N40}$	4%(*s*) + 96%(*p*)	C32–N39	π*	52.1
	$(LP2)_{N40}$	29%(*s*) + 71%(*p*)	Pt27–P25	σ*	111.6
Back-Donation	$(LP1)_{Pt27}$	97%(*d*)	Pt27–P25	σ*	23.2
	$(LP1)_{Pt27}$	97%(*d*)	Pt27–S28	σ*	26.5

Table 8. Second-order perturbation energies ($E^{(2)}$) for charge transfers from donor to acceptor orbitals in $[Pt(BPT)(PPh_3)_2]$ (**5**).

	Donor	Type	Acceptor	Type	$E^{(2)}$
Donation	$(LP2)_{S65}$	100%(*p*)	C67–N79	π*	18.0
	$(LP1)_{N66}$	4%(*s*) + 96%(*p*)	C67–N79	π*	54.8
	$(LP2)_{N66}$	31%(*s*) + 69%(*p*)	Pt64–P1	σ*	112.2
	$(LP1)_{N79}$	33%(*s*) + 67%(*p*)	C67–S65	σ*	24.3
	$(LP1)_{P30}$	55%(*s*) + 45%(*p*)	Pt64–S65	σ*	152.0
	Pt64–P1	Σ	Pt64–S65	σ*	22.1
	Pt64–S65	Σ	Pt64–P1	σ*	46.8
Back-Donation	$(LP1)_{Pt64}$	4%(*s*) + 96%(*d*)	Pt64–P1	σ*	26.8
	$(LP1)_{Pt64}$	4%(*s*) + 96%(*d*)	Pt64–S65	σ*	28.7

Table 9. Second-order perturbation energies ($E^{(2)}$) for charge transfers from donor to acceptor orbitals in [Pt(BPT)(Bipy)] (**7**).

	Donor	Type	Acceptor	Type	$E^{(2)}$
Donation	$(LP1)_{N4}$	30%(*s*) + 70%(*p*)	Pt21–S22	σ*	105.8
	$(LP1)_{N12}$	30%(*s*) + 70%(*p*)	Pt21–S23	σ*	108.0
	$(LP1)_{N68}$	26%(*s*) + 74%(*p*)	C25–N53	σ*	20.9
	$(LP1)_{N26}$	1%(*s*) + 99%(*p*)	C24–N41	π*	54.2
	$(LP1)_{N41}$	27%(*s*) + 73%(*p*)	C24–N26	σ*	19.0
	$(LP1)_{N53}$	5%(*s*) + 95%(*p*)	C25–N68	π*	42.2
Back-Donation	$(LP1)_{Pt21}$	6%(*s*) + 94%(*d*)	Pt21–S23	σ*	10.5
	$(LP1)_{Pt21}$	6%(*s*) + 94%(*d*)	Pt21–S22	σ*	10.0

Furthermore, Figures 4–6 illustrate donor and acceptor orbitals for the two highest second-order perturbation energies graphically. In line with the previous discussion, these results show that P atoms are very good electron donors to the Pt bonding orbitals. The $E^{(2)}$ values for P donors to Pt acceptor are higher than 150 kcal.mol^{-1}. The next level of the $E^{(2)}$ values belongs to the N donor and anti-bonding orbital of Pt–P or Pt–S as the electron acceptor. In addition to the donation, there is some back-donation in which charges transfer from a central Pt atom to the anti-bonding orbitals of Pt–P and Pt–S. Apparently, this charge back-donation stabilizes the complexes in the range of 10–20 kcal.mol^{-1}. It is interesting to note that the stabilization due to the charge back-donation is higher in complexes (**1**) and (**5**) compared to complex (**7**). This indicates that the probability of charge back-donation is twice in complexes (**1**) and (**5**) compared to complex (**7**).

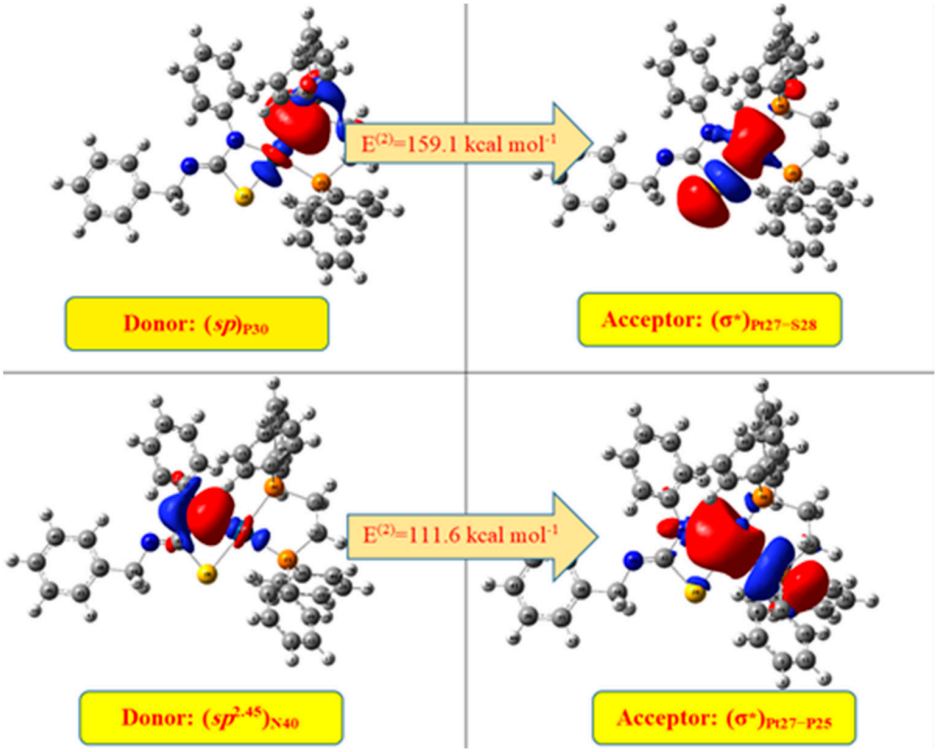

Figure 4. Donor and acceptor orbitals of two highest second-order perturbation energies ($E^{(2)}$) of [Pt(BPT)(dppe)] (**1**) complex.

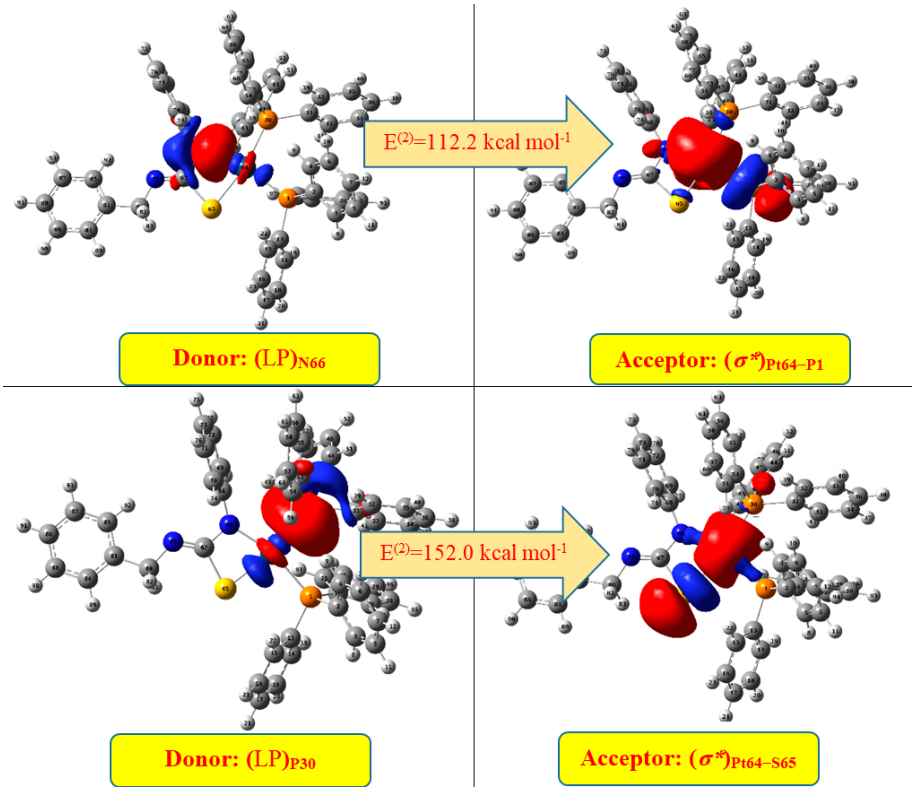

Figure 5. Donor and acceptor orbitals of two highest second-order perturbation energies ($E^{(2)}$) of [Pt(BPT)(PPh_3)$_2$] (**5**) complex.

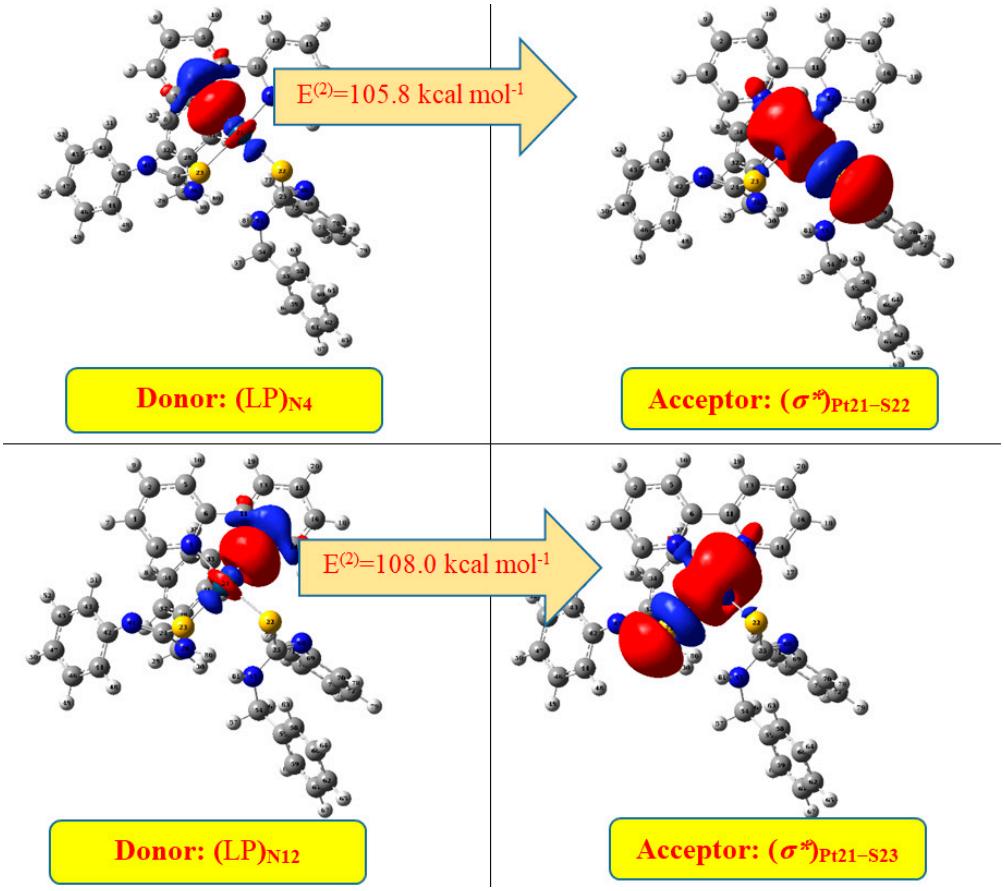

Figure 6. Donor and acceptor orbitals of two highest second-order perturbation energies ($E^{(2)}$) of [Pt(BPT)(Bipy)] (**7**) complex.

2.4.3. MEP Analysis

The molecular electrostatic potentials (MEP) of three selective complexes were calculated from the formatted checkpoint file. To complete this analysis, the total electronic density was considered for the MEP calculation, where the results are shown in Figure 7. In this figure, the charge distribution is represented by a range of colors. The red color is for negative MEP, illustrating the electron-rich regions, and the blue color is for positive MEP showing the regions of electron deficiency. The electron-rich regions favor nucleophilic reactions, and the regions with electron deficiency are prompt for electrophilic reactions. In this calculation, the highest positive and negative values of MEP were fixed in the range of −0.04 to +0.04. The computed images allowed the complexes to be visually compared to understand their properties. Figure 7 shows that all three complexes have bold red color regions, which can act as strong nucleophiles. However, only the dsm-6 complex can play the role of strong electrophile. In these complexes, the thiourea ligand is nucleophilic, and bipyridine is located in the electrophilic center.

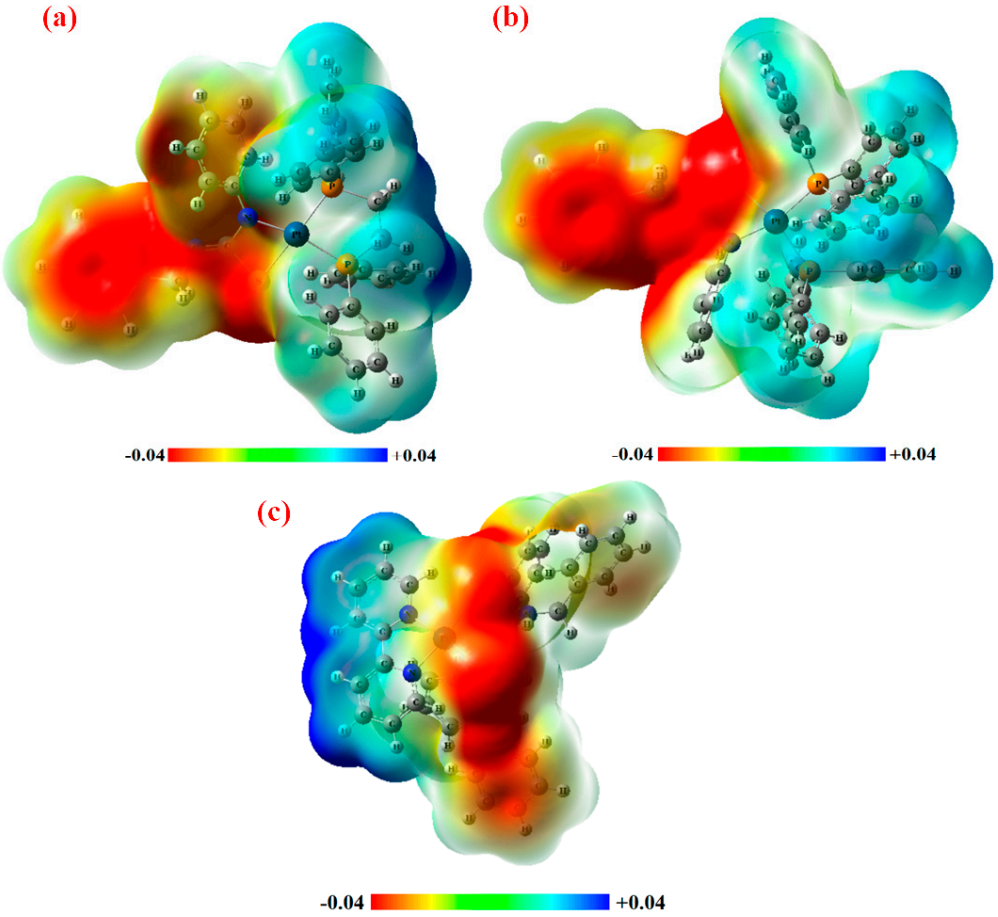

Figure 7. Molecular electrostatic potentials calculated at the level of B3LYP/Def2-TZVP for (**a**) [Pt(BPT)(dppe)] (**1**), (**b**) [Pt(BPT)(PPh_3)$_2$] (**5**), and (**c**) [Pt(BPT)$_2$(Bipy)] (**7**).

3. Experimental Section

3.1. Synthesis of 1-Benzyl-3-phenylthiourea (H_2BPT)

The ligand 1-benzyl-3-phenylthiourea (H_2BPT) was prepared by a modified method described previously [33,34]. In brief, this ligand was prepared by adding 2.14 mL of phenylmethanamine (20 mmol) in 10 mL of benzene under stirring for 10 min. Subsequently, 2.70 mL of isothiocyanatobenzene (20 mmol) was added to the mixture, which was then equilibrated for 4 h. Finally, the mixture was recrystallized with hot ethanol to produce a white precipitate, i.e., 1-benzyl-3-phenylthiourea (yield: 5.27 g or 85%, m.p. = 186–188 °C).

3.2. Synthesis of the Complexes (**1**–**7**)

The complexes (**1**–**7**) were synthesized by following the general procedure, which included the reaction of [$PtCl_2$(diphos)] or, [$PtCl_2$(PPh_3)$_2$] or [PCl_2(diamine)] (0.05 mmol) in $CHCl_3$ (10 mL) with the H_2BPT/NaOH ligand (0.10 mmol) dissolved in ethanol in a (1:2) molar ratio using $CHCl_3$/EtOH as mixed solvents (1:1). The reaction mixture was stirred and refluxed for 2 h, which gave pale yellow solution. Microscale crystals of the targeted complexes were obtained upon slow evaporation of the reacted solution.

3.3. Molecular Calculations

Three different complexes were selected to study theoretically by molecular simulation. The structures of [Pt(BPT)(dppe)] (**1**), [Pt(BPT)(PPh_3)$_2$] (**5**), and [Pt(BPT)(Bipy)] (**7**) complexes were optimized with the B3LYP/Lanl2dz level of theory by using Gaussian 09 program [35]. The frequency analyses were carried out to ensure the optimized structures were in the local points of potential energy surfaces. The number of the imaginary frequency was set at zero in all optimized structures. All post-processing calculations

were obtained using the B3LYP/Def2-TZVP level theory. The electrostatic potential (**ESP**) was calculated from the formatted checkpoint file at the iso-surface value of 0.02, and the density of 0.0004 e/Å^3. Natural bond orbital (**NBO**) calculations, such as natural charges and donor-acceptor stabilization energy, were carried out using the NBO 6.0 program [36]. The GaussView program [37] was used to show the contour plot of HOMO (the highest occupied molecular orbital) and LUMO (the lowest unoccupied molecular orbital).

4. Conclusions

The present work describes the synthesis of a series of phosphine-Pt(II) complexes containing the dianionic thiourea ligand, which was synthesized by reacting one mole of precursor chloro complex, [$PtCl_2$(L-L)] (L-L = dppe, dppp, dppb, dppf, Phen and Bipy) or [$PtCl_2(PPh_3)_2$] with two moles of 1-benzyl-3-phenylthiourea (H_2BPT) in the presence of NaOH as a base. The complexes have been fully characterized by the CHN analysis and NMR, IR, and UV–visible techniques. The spectroscopic results showed that the H_2BPT ligand coordinates in the bidentate fashion through N and S atoms with Pt(II) ion. The cytotoxicity study against the MCF-7 cancer cells was carried out and indicated that [Pt(BPT)$_2$(Bipy)] (**7**) exhibited an anti-cancer property. DFT calculations were also performed under the property of complexes [Pt(BPT)(dppe)] (**1**), [Pt(BPT)$(PPh_3)_2$] (**5**), and [Pt(BPT)$_2$(Bipy)] (7). The calculation results support the spectroscopic results and indicate that these complexes adopt a square planar geometry. However, the exact geometries are distorted square planar due to the different Pt-P and Pt-S bond lengths. In addition, the HOMO–LUMO energy gap calculations showed similar energy gap values between complexes (**1**) and (**5**) but very low values in complex (**7**), which may be a good candidate for photo-catalyst material.

Supplementary Materials: The following supporting information can be downloaded at: https://www.mdpi.com/article/10.3390/inorganics11030125/s1 Figure S1: ^{1}H nmr spectrum of H_2BPT ligand, Figure S2: ^{1}H nmr spectrum of complex **1**, Figure S3: ^{1}H nmr spectrum of complex **2**, Figure S4: ^{1}H nmr spectrum of complex 3, Figure S5: ^{1}H nmr spectrum of complex **4**, Figure S6: ^{1}H nmr spectrum of complex **5**, Figure S7: ^{1}H nmr spectrum of complex 6, Figure S8: ^{1}H nmr spectrum of complex **7**, Figure S9: ^{31}P nmr spectrum of complex **1**, Figure S10: ^{31}P nmr spectrum of complex 2, Figure S11: ^{31}P nmr spectrum of complex **3**, Figure S12: ^{31}P nmr spectrum of complex **4**, Figure S13: ^{31}P nmr spectrum of complex **5**, Figure S14: ^{13}C-{^{1}H} nmr spectrum of H_2BPT, Figure S15: ^{13}C-{^{1}H} nmr spectrum of complex (**1**), Figure S16: ^{13}C-{^{1}H} nmr spectrum of complex (**2**), Figure S17: ^{13}C-{^{1}H} nmr spectrum of complex (**6**), Figure S18: ^{13}C-{^{1}H} nmr spectrum of complex (**7**). References [38,39] are cited in the supplementary materials.

Author Contributions: D.S.M., S.A.A.-J., R.B.-A., A.S.F. and A.S.M.A.-J.: Conceptualization; Data curation; Formal analysis; Methodology; Visualization; Writing—original draft; Writing—review and editing. T.A.Y., A.G.A., M.M.A.-K. and B.S.H.: Conceptualization; Funding acquisition and Writing—review and editing. All authors have read and agreed to the published version of the manuscript.

Funding: This research was supported by the Deanship of Scientific Research at Imam Mohammad Ibn Saud Islamic University for funding through the Research Partnership Program (RP-21-09-67).

Data Availability Statement: In the supporting information of this article, you will find the data supporting this study's findings.

Acknowledgments: The authors are grateful to Tikrit University for its support. The authors also extend their appreciation to the Deanship of Scientific Research at Imam Mohammad Ibn Saud Islamic University for funding through the Research Partnership Program (RP-21-09-67).

Conflicts of Interest: The authors declare no conflict of interest.

References

1. Henderson, W.; Nicholson, B.K.; Dinger, M.B.; Bennett, R.L. Thiourea monoanion and dianion complexes of rhodium (III) and ruthenium (II). *Inorg. Chim. Acta* **2002**, *338*, 210–218. [CrossRef]
2. Elhusseiny, A.F.; Eldissouky, A.; Al-Hamza, A.M.; Hassan, H.H. Metal complexes of the nanosized ligand N-benzoyl-N′-(p-amino phenyl) thiourea: Synthesis, characterization, antimicrobial activity and the metal uptake capacity of its ligating resin. *J. Mol. Struct.* **2015**, *1100*, 530–545. [CrossRef]
3. Beyer, L.; Hoyer, E.; Liebscher, J.; Hartmann, H. Formation of complexes with N-acyl-thioureas. *Z. Chem.* **1981**, *21*, 81–91. [CrossRef]
4. Mühl, P.; Gloe, K.; Dietze, F.; Hoyer, E.; Beyer, L. N-Acyl-thioharnstoffe–effektive Extraktionsmittel für die Flüssig-Flüssig-Extraktion von Metallionen. *Z. Chem.* **1986**, *26*, 81–94. [CrossRef]
5. Koch, K.R. New chemistry with old ligands: N-alkyl-and N, N-dialkyl-N′-acyl (aroyl) thioureas in co-ordination, analytical and process chemistry of the platinum group metals. *Coord. Chem. Rev.* **2001**, *216*, 473–488. [CrossRef]
6. Iliş, M.; Bucos, M.; Dumitraşcu, F.; Cîrcu, V. Mesomorphic behaviour of N-benzoyl-N′-aryl thioureas liquid crystalline compounds. *J. Mol. Struct.* **2011**, *987*, 1–6. [CrossRef]
7. Faihan, A.S.; Al-Jibori, S.A.; Al-Janabi, A.S. Novel base-free dianion complexes of Pt (II) and Pd (II) derived from heterocyclic thiourea and tertiary phosphine ligands. *J. Mol. Struct.* **2022**, *1251*, 131966. [CrossRef]
8. Habtu, M.M.; Bourne, S.A.; Koch, K.R.; Luckay, R.C. Competitive bulk liquid membrane transport and solvent extraction of some transition and post-transition metal ions using acylthiourea ligands as ionophores. *New J. Chem.* **2006**, *30*, 1155–1162. [CrossRef]
9. Yuan, Y.F.; Wang, J.T.; Gimeno, M.C.; Laguna, A.; Jones, P.G. Synthesis and characterisation of copper complexes with N-ferrocenoyl-N′-aryl (alkyl) thioureas. *Inorg. Chim. Acta* **2001**, *324*, 309–317. [CrossRef]
10. Zhang, Y.M.; Wei, T.B.; Xian, L.; Gao, L.M. An efficient synthesis of polymethylene-bis-aroyl thiourea derivatives under the condition of phase-transfer catalysis Phosphoru. *Phosphorus Sulphur Silicon Relat. Elem.* **2004**, *179*, 2007–2013. [CrossRef]
11. Eweis, M.; Elkholy, S.S.; Elsabee, M.Z. Antifungal efficacy of chitosan and its thiourea derivatives upon the growth of some sugar-beet pathogens. *Int. J. Biol. Macromol.* **2006**, *38*, 1–8. [CrossRef] [PubMed]
12. Selvakumaran, N.; Ng, S.W.; Tiekink, E.R.; Karvembu, R. Versatile coordination behavior of N, N-di (alkyl/aryl)-N′-benzoylthiourea ligands: Synthesis, crystal structure and cytotoxicity of palladium (II) complexes. *Inorg. Chim. Acta* **2011**, *376*, 278–284. [CrossRef]
13. Gunasekaran, N.; Ng, S.W.; Tiekink, E.R.T.; Karvembu, R. Hypodentate coordination of N, N-di (alkyl/aryl)-N′-acylthiourea derivatives in Cu (I) complexes. *Polyhedron* **2012**, *34*, 41–45. [CrossRef]
14. Saeed, S.; Rashid, N.; Jones, P.G.; Ali, M.; Hussain, R. Synthesis, characterization and biological evaluation of some thiourea derivatives bearing benzothiazole moiety as potential antimicrobial and anticancer agents. *Eur. J. Med. Chem.* **2010**, *45*, 1323–1331. [CrossRef]
15. Hochreuther, S.; Puchta, R.; van Eldik, R. Thermodynamic and kinetic studies on novel dinuclear platinum (II) complexes containing bidentate N, N-donor ligands. *Inorg. Chem.* **2011**, *50*, 8984–8996. [CrossRef]
16. Jarzynka, P.; Topolski, A.; Uzarska, M.; Czajkowski, R. New dinuclear platinum complexes. Synthesis and kinetics of chloride substitution by thiourea and glutathione in water–DMF solution. *Inorg. Chim. Acta* **2014**, *413*, 60–67. [CrossRef]
17. Al-Janabi, A.M.; Faihan, A.S.; Al-Mutairi, A.M.; Hatshan, M.R.; Al-Jibori, S.A.; Al-Janabi, A.S. Spectroscopic, biological activity studies, and DFT calculations, of Pd (II) and Pt (II) complexes of 4-Methylene-3-phenyl-3, 4-dihydroquinazoline-2 (1H)-thione. *J. Indian Chem. Soc.* **2022**, *99*, 100774. [CrossRef]
18. Mihai, S.; Negoiu, M. Synthesis Characterization and Antitumor Activity of Platinum (II), Palladium (II), Gold (III), Silver (I), Copper (II), Rhodium (III) and Ruthenium (III) Complexes with N-Antipirine-N′-Benzoylthioureea. *Rev. Chim.* **2012**, *63*, 697–702.
19. Geary, W.J. The use of conductivity measurements in organic solvents for the characterization of coordination compounds. *Coord. Chem. Rev.* **1971**, *7*, 81–122. [CrossRef]
20. Faihan, A.S.; Hatshan, M.R.; Alqahtani, A.S.; Nasr, F.A.; Al-Jibori, S.A.; Al-Janabi, A.S. New divalent metal ion complexes with 1, 8-diaminonapthalene-2-thione: Synthesis, Spectroscopic, anti-bacterial and anticancer activity studies. *J. Mol. Struct.* **2022**, *1247*, 131291. [CrossRef]
21. Al-Mouqdady, O.D.; Al-Janabi, A.S.; Hatshan, M.R.; Al-Jibori, S.A.; Fiahan, A.S.; Wagner, C. Synthesis, characterization, anti-bacterial and anticancer activities of Palladium (II) mixed ligand complexes of 2-mercapto-5-methyl-1, 3, 4-thiadiazole (HmtzS) and phosphines. Crystal structure of [Pd (mtzS) 2 (dppf)]. H_2O. EtOH. *J. Mol. Struct.* **2022**, *1264*, 133219. [CrossRef]
22. Al-Mouqdady, O.D.; Hatshan, M.R.; Fiahan, A.S.; Alheety, M.A.; Al-Janabi, A.S. Mercury (II)-complex with 5-methyl-1, 3, 4-thiadiazole-2-thiol: Kinetic studies of hydrogen storage. *Int. J. Hydrog. Energy* **2022**, *47*, 24852–24860. [CrossRef]
23. Jensen, K.A.; Nielsen, P.H. Infrared Spectra of Some Organic Compounds of Group VB Elements. *Acta Chem. Scand.* **1963**, *17*, 1875. [CrossRef]
24. Al-Janabi, A.S.; Al-Samrai, O.A.A.; Yousef, T.A. New palladium (II) complexes with 1-phenyl-1H-tetrazole-5-thiol and diphosphine Synthesis, characterization, biological, theoretical calculations and molecular docking studies. *Appl. Organomet. Chem.* **2020**, *34*, e5967. [CrossRef]
25. Al-Janabi, A.S.; Al-Samra, U.A.A.; Othman, E.A.; Yousef, T.A. Optical properties, structural, and DFT studies of Pd (II) complexes with 1-phenyl-1H-tetrazol-5-thiol, X-ray crystal structure of [Pd (κ1-S-ptt) 2 (κ2-dppe)] complex. *Appl. Organomet. Chem.* **2020**, *34*, e5996. [CrossRef]

26. Al-Jibori, S.A.; Al-Janabi, A.S.; Al-Sahan, S.W.; Wagner, C. Pd (II)-pyrrolidine dithiocarbamate complexes: Synthesis, spectroscopic studies and molecular structure of [Pd (PyDT)(ppy)]. *J. Mol. Struct.* **2021**, *1227*, 129524. [CrossRef]
27. Al-Janabi, A.S.; Kadhim, M.M.; Al-Nassiry, A.I.; Yousef, T.A. Antimicrobial, computational, and molecular docking studies of Zn (II) and Pd (II) complexes derived from piperidine dithiocarbamate. *Appl. Organomet. Chem.* **2021**, *35*, e6108. [CrossRef]
28. Faihan, A.S.; Aziz, N.M.; Ashfaq, M.; Hassan, W.M.; Al-Jibori, S.A.; Al-Janabi, A.S.; Al-barwari, A.S. Synthesis, characterization, and x-ray crystallography of unexpected chloro-substitution on 1-(4-chlorophenyl)-3-phenylthiourea platinum (II) complex with tertiary phosphine ligand. *J. Mol. Struct.* **2022**, *1270*, 133985. [CrossRef]
29. Miessler, G.L.; Donald, T.A. Coordination Chemistry III: Electronic Spectra. In *Inorganic Chemistry*, 5th ed.; Pearson Education: Upper Saddle River, NJ, USA, 2004; pp. 417–428.
30. El-Sayed, M.A.A.; El-Husseiny, W.M.; Abdel-Aziz, N.I.; El-Azab, A.S.; Abuelizz, H.A.; Abdel-Aziz, A.A.M. Synthesis and biological evaluation of 2-styrylquinolines as antitumour agents and EGFR kinase inhibitors: Molecular docking study. *J. Enzym. Inhib. Med. Chem.* **2018**, *33*, 199–209. [CrossRef] [PubMed]
31. Faihan, A.S.; Al-Jibori, S.A.; Hatshan, M.R.; Al-Janabi, A.S. Antibacterial, spectroscopic and X-ray crystallography of newly prepared heterocyclic thiourea dianion platinum (II) complexes with tertiary phosphine ligands. *Polyhedron* **2022**, *212*, 115602. [CrossRef]
32. Appleton, T.G.; Clark, H.C.; Manzer, L.E. The trans-influence: Its measurement and significance. *Coord. Chem. Rev.* **1973**, *10*, 335–422. [CrossRef]
33. Faihan, A.S.; Hatshan, M.R.; Kadhim, M.M.; Alqahtani, A.S.; Nasr, F.A.; Saleh, A.M.; Al-Janabi, A.S. Promising bio-active complexes of platinum (II) and palladium (II) derived from heterocyclic thiourea: Synthesis, characterization, DFT, molecular docking, and anti-cancer studies. *J. Mol. Struct.* **2022**, *1252*, 132198. [CrossRef]
34. Al-Jibori, S.A.; Dayaaf, N.A.; Mohammed, M.Y.; Merzweiler, K.; Wagner, C.; Hogarth, G.; Richmond, M.G. cis–trans Isomerism at Square-Planar MN2S2 Centers (M = Pd, Pt): Crystal Structures of N-Phenyl-N-(2-thiazoyl) thiourea Complexes trans-Pd (S2N3C10H8) 2 and cis-Pt (S2N3C10H8) 2 and Density Functional Calculations. *J. Chem. Crystallogr.* **2013**, *43*, 365–372. [CrossRef]
35. Frisch, M.J.; Trucks, G.W.; Schlegel, H.B.; Scuseria, G.E.; Robb, M.A.; Cheeseman, J.R.; Scalmani, G.; Barone, V.; Mennucci, B.; Petersson, G.A.; et al. *Fox, Gaussian 09 Rev. E.01*; Gaussian, Inc.: Wallingford, CT, USA, 2009.
36. Glendening, E.D.; Landis, C.R.; Weinhold, F. NBO 6.0: Natural bond orbital analysis program. *J. Comput. Chem.* **2013**, *34*, 1429–1437. [CrossRef] [PubMed]
37. Dennington, R.; Keith, T.; Millam, J. *GaussView, Version 5.0*; Semichem Inc.: Shawnee Mission, KS, USA, 2016.
38. Price, J.H.; Williamson, A.N.; Schramm, R.F.; Wayland, B.B. Palladium(II) and Platinum(II) Alkyl Sulfoxide Complexes. Examples of Sulfur-Bonded, Mixed Sulfur and Oxygen-Bonded, and Totally Oxygen-Bonded Complexes. *Inorg. Chem.* **1972**, *11*, 1280–1284. [CrossRef]
39. Abdullah, B.H.; Abdulla, M.A.; Al-Jibori, S.A.; Al-Allaf, T.A.K. Platinum(II) Linkage Isomeric Complexes Containing Mixed Ligands 4,5-diphenyl-1,2,4-triazole-3-thione and Diphosphines Ph2P(CH2)nPPh2 (n = 1,2 or 3). *Asian J. Chem.* **2007**, *19*, 1334.